

Bayesian Nonparametric Cost-Effectiveness Analyses: Causal Estimation and Adaptive Subgroup Discovery

[Preliminary Working Draft]

Arman Oganisian * ¹, Nandita Mitra¹, and Jason A. Roy ²

¹University of Pennsylvania

Division of Biostatistics

Department of Biostatistics, Epidemiology, and Informatics

²Rutgers University

Department of Biostatistics and Epidemiology

June 16, 2022

Abstract

Cost-effectiveness analyses (CEAs) are at the center of health economic decision making. While these analyses help policy analysts and economists determine coverage, inform policy, and guide resource allocation, they are statistically challenging for several reasons. Cost and effectiveness are correlated and follow complex joint distributions which are difficult to capture parametrically. Effectiveness (often measured as increased survival time) and cost both tend to be right-censored. Moreover, CEAs are often conducted using observational data with non-random treatment assignment. Policy-relevant causal estimation therefore requires robust confounding control. Finally, current CEA methods do not address cost-effectiveness heterogeneity in a principled way - opting to either present marginal results or cost-effectiveness results for pre-specified subgroups. Motivated by these challenges, we develop a nonparametric Bayesian model for joint cost-survival distributions in the presence of censoring. Our approach utilizes an Enriched Dirichlet Process prior on the covariate effects of cost and survival time, while using a separate Gamma Process prior on the baseline survival time hazard. Causal CEA estimands are identified and estimated via a Bayesian nonparametric g-computation procedure. Finally, we propose leveraging the induced clustering of the Enriched Dirichlet Process to adaptively discover subgroups of patients with different cost-effectiveness profiles. We outline an MCMC procedure for full posterior inference, evaluate frequentist properties via simulations, and apply our model to an observational study of endometrial cancer therapies using medical claims data.

*Corresponding author. Email: aoganisi@upenn.edu.

1 Introduction

Cost-effectiveness analyses (CEAs) are ubiquitous in public health policy and health economics research, with use-cases ranging from treatment comparison to determining drug coverage and informing policy more broadly. Though important, CEAs remain statistically challenging for several reasons. First, cost and effectiveness are often correlated, with joint distributions typically exhibiting extreme skewness and multimodality. In these settings, parametric models that impose strong distributional, linearity, and additivity constraints are not tenable. Second, in many cases effectiveness is operationalized as survival time - which is prone to right-censoring if subjects drop out before the end of the study. For such patients, we only observe a lower bound on their survival time and accumulated costs. Third, CEAs are often conducted using observational data. Though observational studies are less expensive and data are readily available, they are prone to confounding. Valid estimation of CEA contrasts requires statistical adjustment - so that differences in cost-effectiveness due to treatment can be differentiated from differences due to confounders.

The early statistical literature [1, 2, 3, 4] focused on cost estimation, while assuming efficacy was constant between treatments. Cost estimation alone is challenging due to the pathological nature of costs (censoring, skewness, zero-inflation, etc). Our work enhances this literature by developing a joint model for cost and survival time, rather than solely focusing on cost. Previous work on such joint models have been published [5, 6, 7, 8]. These approaches decompose the joint distribution into a product of a marginal survival time distribution and a cost distribution conditional on survival time. Huang et al. refer to this as a “calibration regression” approach. Handorf et al. and Huang et al. approach the modeling from a frequentist point of view. While the former uses a fully parametric approach, Huang et al. use a semi-parametric approach - making only first and second moment assumptions. Baio et al. took a fully parametric Bayesian approach to joint modeling that did not allow for full covariate adjustment. In contrast, our Bayesian joint modeling approach makes neither strong distributional assumptions nor functional form (linearity, additivity) assumptions and allows for covariate adjustment.

Li et al [3] took a significant step toward robust causal inference in cost-effectiveness. They formulated causal CEA contrasts in terms of potential outcomes and develop a doubly-robust estimation approach that combined separate conditional mean models for cost and survival with a treatment propensity score model. They show that CEA contrasts can be estimated consistently if either the propensity score or cost/survival regressions are correct. We build on this work in several ways. Like Li et al, we also formulate CEA contrasts in terms of potential outcomes - endowing these contrasts with explicitly causal interpretations. However, our modeling approach is fully nonparametric and, therefore, more flexible than the doubly-robust estimator. Moreover, our approach is a Bayesian model for the full joint cost-effectiveness distribution (not a combination of separate mean models). While the doubly robust approach targets net monetary benefits specifically, our approach yields posterior inference for any estimand that is a function of the joint distribution. Finally, our approach allows for covariate-dependent censoring. Though Li et al. mention an extension to covariate-dependent censoring, their application of interest and simulation studies are under random censoring.

Lastly, our work advances the literature in Bayesian nonparametric (BNP) causal inference. While an array of nonparametric priors have been successfully applied to causal inference [9, 10, 11, 12, 13, 14], modeling of bivariate counterfactual outcomes using the Enriched Dirichlet Process (EDP) and Gamma process (GP) has not been explored. Importantly, our model allows for adaptive discovery of subgroups that may have heterogenous cost-effectiveness profiles. In CEAs, heterogenous effects are typically either ignored in favor of a single, marginal effect or explored along pre-defined subgroups (e.g. hispanic males). Methods for estimating heterogenous treatment effects using Bayesian Additive Regression Trees (BART) [15, 16] and Causal Forests

[17] have been proposed which are distinct from our approach in several ways. These methods focus on individual-level treatment effects. Instead, our goal is to discover *subgroups* with heterogenous individual treatment effects (ITEs). While Athey et al. [17] use their method to find heterogenous subgroups, these subgroups were pre-defined. Specifically, they observe data on students nested within schools and they attempt to determine whether treatments were heterogenous across schools. In contrast, our approach does not require pre-specification of the subgroups (i.e., schools). We use the induced clustering property of the EDP to find these subgroups in a probabilistically principled way. Once found, we can then describe these subgroups in terms of observed covariates. The cited methods instead use a bottom-up approach to characterizing variation in ITEs: trying to group the individual-level treatment effects using heuristic post-hoc procedures. For instance, Henderson et al. [16] regress the estimated ITEs on observed covariates using weighted least squares and look for large coefficients to indicate “drivers” of heterogeneity.

Our approach decomposes the full joint cost-effectiveness distribution into a survival distribution, and a cost model conditional on survival time. We specify a “local” parametric cost model and a proportional hazard survival model. A Gamma Process prior is placed on the baseline hazard while an EDP prior is placed on the joint distribution of the cost and survival covariate effects. A key property of the EDP is its induced posterior clustering. The EDP probabilistically partitions the dataset into clusters with similar cost-effectiveness covariate effects and associates different “local” models with each cluster. Thus, the joint posterior model for cost-effectiveness is an adaptive mixture of locally parametric models. It is adaptive in the sense that the number of clusters need not be pre-specified. As many clusters are introduced as the complexity of the cost-effectiveness distribution demands.

In the remaining sections, we provide a brief overview of cost-effectiveness and the relevant target estimands. We then present our model, complete with a Markov Chain Monte Carlo (MCMC) algorithm for posterior inference. We propose incorporating our model into a g-computation framework for posterior causal effect estimation. Lastly, we outline how the induced clustering of the EDP can be used to discover subgroups of patients with different cost-effectiveness profiles. We propose a Differential Subgroup Index (*DSI*) for assessing quality of the EDP cost-effectiveness partitions. We end with simulation studies assessing frequentist properties of our causal effect estimates and an application to endometrial cancer therapies using observational insurance claims data.

2 Overview of Relevant Cost-Effectiveness Contrasts

In this paper, we consider a binary treatment setting where assignment is indicated by $A \in \{0, 1\}$. The goal of CEAs is to characterize the relative cost-effectiveness of these two treatments - necessitating both a cost and efficacy measure. In many settings, the total cost, Y , includes all costs accumulated under this treatment - e.g., hospitalization and medication costs incurred due to adverse events of the treatment. Moreover, costs are typically measured in inflation-adjusted dollars from the *payer’s* perspective - not the patient’s perspective. In single-payer systems like that of the United Kingdom, this would be the National Health Service (NHS). For older patients in the United States, the payer of interest in most policy-oriented CEAs is Medicare. Though lifetime costs is often of interest, many CEAs set a duration for cost accrual (e.g. 2-year costs) due to follow-up constraints. In this paper, we consider a survival time effectiveness measure, T . This is the dominant effectiveness measure in cancer CEAs, the motivating data application of our paper. It is especially complicated as survival time is often right-censored either by loss to follow up or study termination.

A typical CEA observational study follows patients after diagnosis and assignment to one of two treatment

regimes. After some follow-up period, everyone’s (possibly censored) cost and survival time are recorded and various cost-effectiveness contrasts can then be computed. For instance, the incremental cost effectiveness ratio (ICER) is given as $ICER = \frac{E[Y|A=1] - E[Y|A=0]}{E[T|A=1] - E[T|A=0]}$. This measures the average cost per unit of effectiveness (increase in survival time). We can also define a monetary value under each treatment, $MV(\kappa) = Y\kappa - T$. Here, κ is the “willingness-to-pay” parameter. It is interpreted as the maximum dollar value the payer is willing to give for a one unit increase in effectiveness. It is considered a fixed, user-specified value. Here, we will suppress notational dependence on κ by simply writing MV where there is no ambiguity. Health economists often assess cost-effectiveness via the net monetary benefit, $NMB = E[MV | A = 1] - E[MV | A = 0]$, where we have again suppressed dependence of NMB on κ . This contrast is closely related to $ICER$ and can be interpreted as the average difference in monetary value between treatment groups. Another related quantity is the Cost Effectiveness Acceptability Curve (CEAC), which is a curve comprised of $P(NMB > 0)$ plotted for various κ . Valid causal estimation of these contrasts requires, among other things, adjustment for confounders. However, even if all relevant confounders are measured and included in the model, misspecification of the adjustment model may yield biased estimates of cost-effectiveness contrasts. This motivates the need for robust nonparametric modeling.

3 Joint Model for Cost and Survival Time

We consider a binary treatment setting in which n patients are assigned to treatment $A_i \in \{0, 1\}$ at baseline and followed up for some finite time. We observe data $D = \{Y_i, T_i, X_i, \delta_i\}_{i=1:n}$ from this study. Here, $X_i = (A_i, L_i)$ is a covariate vector that contains the treatment indicator and q binary or continuous pre-treatment confounders, L_i . For notational convenience, we proceed without an intercept, but note that a 1 can be included in the first entry of X_i if desired. We let T_i be the right-censored survival time. We also let $\delta_i = 1$ indicate that T_i is a death as opposed to censoring time. Patients may be censored due to loss to followup or due to surviving past study termination. Finally, $Y_i \in \mathcal{Y}$ denotes cost accumulated through time T_i . Note that the joint distribution can be factored into a survival time distribution and cost distribution conditional on time. A joint model follows from specifying “local” models for these two distributions

$$\begin{aligned} Y_i | T_i, X_i, \omega_i &\sim p(Y_i | X_i, T_i, \omega_i) \\ T_i | X_i, \theta_i, \lambda_0 &\sim \lambda_0(t) \exp(X_i' \theta_i) \\ \omega_i, \theta_i | G &\sim G. \end{aligned} \tag{3.1}$$

Conditional on time, cost follows some local distribution $p(Y_i | X_i, T_i, \omega_i)$ governed by parameters ω_i . Survival time follows some local hazard function which is parameterized as having some baseline hazard, λ_0 (implicitly a function of t) with covariate effects, θ_i , multiplying this baseline hazard. Lastly, ω_i and θ_i - the covariate effects of the cost and effectiveness model - both follow some joint prior distribution G , which is unknown. Choice of the local models are application-specific but are not crucial for model fit, as will become apparent when we discuss the nonparametric priors used for G and λ_0 .

One consideration when choosing the local model is desired predictive support. If costs are sufficiently far away from zero, then having $\mathcal{Y} = (-\infty, \infty)$ and setting $p(Y_i | X_i, T_i, \omega_i)$ to be Gaussian with mean and variance $\omega_i = (\mu_i, \phi_i)$ and regression $\mu_i = (T_i, X_i)' \beta_i$ will fit adequately. If the non-negative nature of costs must be respected we can have $\mathcal{Y} = (0, \infty)$ and set the local model to a log-Normal distribution. For applications with zero-inflated costs, we may wish to explicitly put positive support on zero - i.e. setting $\mathcal{Y} = \{0\} \cup (0, \infty)$.

This can be done by specifying a two-part model $Y_i | T_i, X_i, \omega_i \sim \pi_i \delta_0(Y_i) + (1 - \pi_i) f(Y_i | T_i, X_i, \beta_i)$, where $\pi_i = P(Y_i = 0 | T_i, X_i, \gamma_i)$ is a covariate-dependent model for the probability of cost being zero and δ_0 is the point mass distribution at 0. In this case, the cost parameter vector is $\omega_i = (\gamma_i, \beta_i)$. Oganisian et al. [18] developed a nonparametric Bayesian estimation procedure for this two-part model, where f could be either log-Normal or Normal.

In Model (3.1), censored patients contribute to the likelihood through both models. In the hazard model, they contribute to the likelihood through the survival function in the usual way. In the cost model, censored patients contribute by providing information on the distribution of costs accumulated up to the time of censoring. The former requires that censoring of survival time be random given covariates X_i . This is a standard assumption in survival analysis. The latter requires that censoring at a particular time be independent of cost, conditional on covariates. That is, $Y_i \perp \delta_i | X_i, T_i$. This is similar to Lin’s “extended assumption of independent censoring” [1]. It allows us to learn the conditional cost distribution, $p(Y | T, X)$, from both censored and uncensored subjects, while allowing for covariate-dependent censoring.

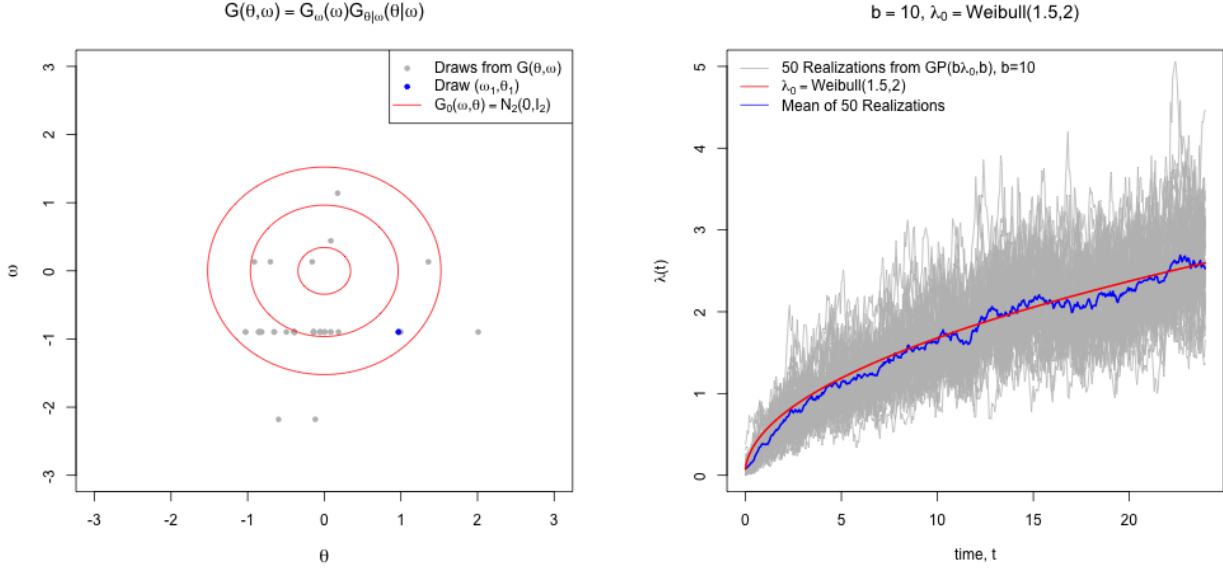
3.1 Nonparametric Priors

We specify the following nonparametric priors on the unknown model quantities, G and λ_0 .

$$\begin{aligned} G | \alpha_\omega, \alpha_\theta &\sim EDP(\alpha_\omega, \alpha_\theta, G_0) \\ \lambda_0 | b, \lambda_0^*, \xi &\sim \mathcal{GP}(b\lambda_0^*, b, \xi), \end{aligned} \tag{3.2}$$

Above, EDP denotes the Enriched Dirichlet Process [19] prior on G and \mathcal{GP} denotes the dependent Gamma Process prior [20] on the baseline hazard λ_0 . These priors are nonparametric in the sense that they are distributions of infinite-dimensional objects - the former over probability distributions and the latter over hazard functions. Realizations, G , from the EDP are discrete probability distributions centered around a base distribution $G_0(\omega_i, \theta_i) = G_{0\omega}(\omega_i)G_{0\theta|\omega}(\theta_i|\omega_i)$ with two concentration parameters, α_ω and α_θ . Some prior realizations are visualized in Figure 1a. Just as with the Dirichlet Process (DP), this discreteness induces a posterior clustering of patients. Unlike the DP, the clustering induced by the EDP is nested. *A posteriori*, patients with similar cost parameters are clustered together into what we call ω -clusters. Within each ω -cluster, patients with similar effectiveness parameters are clustered together (θ -clusters). The EDP prior does not require pre-specification of the number of clusters. The clustering is data-adaptive, with as many clusters being introduced as needed to capture the complexity of the cost-effectiveness distribution. The posterior model for the joint distribution is therefore an adaptive nested mixture of cost-effectiveness models - with each component model having the form of the local model in (3.1), but with different component-specific parameters. In the machine learning literature, these models are often referred to as “mixture of experts” learners: the data space are partitioned into homogenous regions, each having its own model that develops “expertise” in that region. This is in contrast to ensemble learners (e.g. BART and Random Forests), which apply multiple models to the *entire* data and combine the results post-hoc.

The dependent Gamma process can be thought of as a prior over the space of hazard functions. Each realization λ_0 from the \mathcal{GP} is a hazard function centered around a mean function λ_0^* with concentration parameter b . Some prior realizations are visualized in Figure 1b. The process is “dependent” in that it induces a prior AR(1) autocorrelation structure on λ_0 : the hazard at time point t is a weighted average of the hazard at the previous time point and the prior hazard, λ_0 . The induced AR(1) smoothness, controlled by hyperparameter ξ , regularizes the empirical estimate of the baseline hazard - which can be quite erratic at



(a) 100 draws of $(\theta, \omega) \sim G$ where $G \sim EDP(10, 10, N_2(0, I_2))$. Note the nested discreteness of G causes ties among the draws: there are 31 other draws with the same ω value as the blue point, but with different θ values.

(b) Gray lines show 50 hazard realizations from a gamma process centered around the hazard of a *Weibull*(1.5, 2) distribution. The blue line shows the mean of the 50 realizations.

Figure 1: Realizations of the Enriched Dirichlet and Gamma Processes.

later time points when the at-risk set is small.

These prior choices are motivated by the shortcomings of the standard DP. A potential issue with specifying $G \sim DP(\alpha G_0)$ is that it imposes a single layer of clustering for both cost and effectiveness. Many clusters may be introduced to fit the joint of Y and T if one of these dimensions is more complex - even if the other is very simple. This makes estimates needlessly variable. The nested nature of the *EDP* avoids this by allowing varying number of clusters on each dimension. Thus, it is possible to introduce a single cost cluster that has many survival time subclusters. Similarly, modeling the baseline hazard separately avoids introduction of excess clusters to fit a potentially complicated function which, for causal estimation purposes, is a nuisance. This is also the reason why we opt for a proportional hazard (PH) formulation rather than an accelerated failure time (AFT) approach: PH models clearly separate the covariate effects from the baseline risk - which we do not want influencing the *EDP* mixture.

3.2 Posterior Inference using Markov Chain Monte Carlo

Inference for Model 3.1 is accomplished via MCMC. We follow the general scheme of Neal’s algorithm 8 [21], which proposes data augmentation for sampling DP posteriors. Previous work [14] used this approach to sample *EDP* posteriors, though without a Gamma Process update and no joint outcome considerations. The idea is to introduce latent cluster indicators for each subject. Each MCMC iteration then alternates between updating clustering assignments conditional on parameters and updating cluster-specific parameters conditional on these updated assignments. At iteration m , we may have $J^{(m)}$ occupied ω -clusters indexed by $j \in \{1, \dots, J^{(m)}\}$ and, within the j^{th} ω -cluster, we may have $K_j^{(m)}$ occupied θ -clusters indexed by $k_j \in \{1, \dots, K_j^{(m)}\}$. Let $c_{1:n} = (c_1, \dots, c_n)$ be cluster assignment indicators where each c_i is a vector with first and second entry

indicating membership to an ω -cluster θ -subcluster, respectively. Throughout, we use the notation $v_{a:b}$, where $a < b$ are integers, to denote the collection $(v_a, v_{a+1}, \dots, v_b)$. Similarly, let $\omega_{[j]}$ represent the cost parameter associated with cluster j and $\theta_{[j,k]}$ represent the effectiveness parameter associated with the k^{th} subcluster of ω -cluster j . Moreover, define n_j^{-i} and $n_{j,k}^{-i}$ as the number of subjects (excluding subject i) currently occupying ω -cluster j and ω - θ cluster j, k at the current iteration. At each iteration m we conduct the following sequence of conditional posterior updates:

- *Update cluster membership:*

- Propose parameters for a new θ -subcluster for each existing ω -cluster, $\{\theta_{[j, K_j^{(m)}+1]} : j \in 1, \dots, J^{(m)}\}$.
- Propose parameters for a new ω -cluster with a θ subcluster, $\{\omega_{[J^{(m)}+1]}, \theta_{[J^{(m)}+1, 1]}\}$.
- Conditional on current draws of all cost-effectiveness parameters and $\lambda_0^{(m)}$, update $c_i^{(m)}$ according to the following probabilities:

$$P(c_i^{(m+1)} = (j, k) \mid -, D) \propto \begin{cases} \frac{n_j^{-i} n_{j,k}^{-i}}{n_j^{-i} + \alpha_\theta} p(Y_i, T_i \mid X_i, \omega_{[j]}^{(m)}, \theta_{[j,k]}^{(m)}, \lambda_0^{(m)}) & \text{for existing } j, k \\ \frac{n_j^{-i} \alpha_\theta}{n_j^{-i} + \alpha_\theta} p(Y_i, T_i \mid X_i, \omega_{[j]}^{(m)}, \theta_{[j, K_j^{(m)}+1]}^{(m)}, \lambda_0^{(m)}) & \text{for existing } j, \text{ new } k \\ \alpha_\omega p(Y_i, T_i \mid X_i, \omega_{[J^{(m)}+1]}^{(m)}, \theta_{[J^{(m)}+1, K_j^{(m)}+1]}^{(m)}, \lambda_0^{(m)}) & \text{new } j, k \end{cases}$$

- *Update cluster parameters:* These require Metropolis-Hastings steps if $G_{0\omega}$ or $G_{0\theta|\omega}$ are not conjugate.

- Update each cluster’s cost parameter, $\omega_{[k]}$, by drawing from conditional posterior

$$\omega_{[k]}^{(m+1)} \sim p(\omega_{[k]} \mid c_{1:n}^{(m+1)}, D) \propto G_{0\omega}(\omega_{[k]}) \prod_{i \mid c_i^{(m+1)} \in (k, \cdot)} p(Y_i \mid T_i, X_i, \omega_{[k]})$$

- For each k , update $\theta_{[j,k]}$ by drawing from conditional posterior

$$\theta_{[j,k]}^{(m+1)} \sim p(\theta_{[j,k]} \mid c_{1:n}^{(m)}, \lambda_0^{(m)}, D) \propto G_{0\theta|\omega}(\theta_{[j,k]}) \prod_{i \mid c_i^{(m)} \in (k, j)} p(T_i \mid X_i, \lambda_0^{(m)}, \theta_{[j,k]})$$

- *Update baseline hazard, $\lambda_0^{(m+1)}$:* This is a multi-step update involving a discretization of the time interval, and updating several latent, hierarchical parameters that induce the AR(1) structure. These updates involve a mix of grid sampling and adaptive Metropolis-Hastings. Details are provided in the appendix.

Note that the induced nested clustering of the *EDP* is explicitly encoded into this sampler. In the cluster-update step, a given subject is most likely to be assigned to the cluster with parameters that yield the highest joint-distribution evaluation (i.e. fit their data the best). Moreover, each subject can possibly be assigned to a new cost cluster, new effectiveness cluster within an existing cost cluster, or a new cost-effectiveness cluster. The latter is likely to occur if, for example, the subject is so unique that random parameter draws from the prior fit that subject’s data better than any of the existing cluster-specific parameters. Furthermore, note that each term for an existing cluster in $P(c_i^{(m+1)} = (j, k) \mid -, D)$ is an increasing function of the number of patients already assigned to that cluster. This is the “rich-get-richer” property of the *EDP* - the *a priori* favoring of assignment to larger clusters. This prevents over-fitting by penalizing the addition of many small clusters. After every cycle, $c_i^{(m+1)}$ maps each subject to a set of updated parameters $(\omega_i^{(m+1)}, \theta_i^{(m+1)}, \lambda_0^{(m+1)})$. After a sufficient burn-in period this algorithm produces M draws from the posterior $\{\omega_{1:n}^{(m)}, \theta_{1:n}^{(m)}, \lambda_0^{(m)}, c_{1:n}^{(m)}\}_{1:M}$.

3.3 Prior and hyperparameter choice

We choose an “empirical Bayes” approach to setting hyperparameters due to a number of advantages. It is computationally tractable relative to cross-validation approaches. Moreover, it reigns in the cluster-specific parameters to within a reasonable range of the observed data. This keeps the *EDP* from proposing cluster parameters that are wildly at odds with the observed data. Lastly, it can be used even when we lack substantive prior knowledge about the parameters, which is often the case.

The hyperparameters for the *EDP* are the base distribution $G_0(\omega_i, \theta_i) = G_{0\omega}(\omega_i)G_{0\theta|\omega}(\theta_i|\omega_i)$ and the concentration parameters α_θ and α_ω . Following previous papers [14], we use prior independence so that $G_0(\omega_i, \theta_i) = G_{0\omega}(\omega_i)G_{0\theta}(\theta_i)$. We take an empirical Bayes approach, setting $G_{0\theta}(\theta_i) = N(\hat{\theta}_{PH}, \nu_\theta \hat{C}_{PH})$. Here, we are centering the cluster-specific covariate effects around the Cox proportional hazard estimate, $\hat{\theta}_{PH}$. The prior covariance matrix, \hat{C}_{PH} , is diagonal with the square of the Cox proportional hazard standard error estimates along the diagonal. The parameter ν_θ is a user-specified scalar that controls how tightly or widely dispersed the cluster-specific effects are around the Cox estimates.

The choice of $G_{0\omega}(\omega_i)$ depends on the choice of local cost model. Suppose our local model, $p(Y_i | X_i, T_i, \omega_i)$ is Gaussian, $N(\mu_i, \phi_i)$ with regression $\mu_i = E[Y_i | T_i, X_i] = (T_i, X_i)' \beta_i$ and variance ϕ_i , where β_i is the vector of covariate effects. The full cost parameter vector is $\omega_i = (\beta_i, \phi_i)$ and we could set $G_{0\omega}(\beta_i, \phi_i) = N(\beta_i; \hat{\beta}_{OLS}, \nu_\omega \hat{\Sigma}_{OLS})IG(\phi_i; shape = a_0, scale = \hat{s}^2(a_0 + 1))$. The vector $\hat{\beta}_{OLS}$ is the OLS estimate of the cost regression and $\hat{\Sigma}_{OLS}$ is a diagonal matrix with the square of the OLS standard error estimates along the diagonal. Similarly, the Inverse Gamma prior for ϕ_i is centered around the empirical outcome variance, $\hat{s}^2 = \frac{1}{n-1}(Y_i - \bar{Y})^2$. The user-specified parameter, a_0 , controls how widely the cluster-specific variances are dispersed around the empirical variance, with higher values indicated wider dispersion. Finally, we follow previous approaches [14, 18] and set vague $Gam(1, 1)$ priors on each of the concentration parameters. These parameters can be interpreted as prior sample sizes for the cost and effectiveness clusters and we typically have no prior information or empirical knowledge about these parameters.

For the Gamma process prior, we again recommend an empirical approach using prior predictive draws. Specifically, first plot the Nelson-Aalen hazard estimate using the observed data. On the same plot, overlay several cumulative hazard draws (as in Figure 1b) from $\mathcal{GP}(b\lambda_0^*, b, \xi)$ where λ_0^* is, say, a *Weibull*(v_0, u_0) hazard. Choose v_0, u_0 , such that the draws are within the range of the empirical estimate. This selects a member of the Weibull family that is reasonably consistent with the data. The dispersion parameter b can be set to control how wide the \mathcal{GP} draws are around the empirical estimate. The parameter ξ can be toggled until an adequate level of AR(1) smoothing at later time points is achieved.

4 Posterior Causal Estimation via G-computation

Here we describe a procedure for full posterior inference for various causal estimands. In potential outcomes notation [22], let $MV^a = T^a \kappa - Y^a$ be the monetary value that would have accrued under treatment $A = a$. Thus, $\Psi = E[NMB] = E[MV^1] - E[MV^0]$ is a causal estimand - the average difference in monetary value that would have accrued had everyone in the target population been assigned to treatment 1 versus treatment 0. In general, treatment assignments in observational CEAs are not random. Instead, they are driven by confounders - factors which both influence treatment and cost-effectiveness. Thus, $E[MV^a] \neq E[MV | A = a]$ since those who actually received treatment may not be representative of the target population. Suppose, however, that we observe a set of confounders, L . Then, under mild extensions of standard causal identification assumptions

of ignorability, consistency, and no interference (see Appendix), we identify Ψ using Robins' G-formula [23]

$$\Psi(\omega_{1:n}, \theta_{1:n}, \lambda_0) = \int_{\mathcal{L}} \left(E[MV \mid A = 1, L, \omega_{1:n}, \theta_{1:n}, \lambda_0] - E[MV \mid A = 0, L, \omega_{1:n}, \theta_{1:n}, \lambda_0] \right) dP(L) \quad (4.1)$$

Above, we have explicitly written $\Psi = \Psi(\omega_{1:n}, \theta_{1:n}, \lambda_0)$ as a function of the parameters governing the joint cost-effectiveness distribution. This is to emphasize that a posterior distribution on these parameters induces a posterior on the the causal estimand Ψ . Each term of Ψ can be computed as

$$E[MV \mid A = 1, L, \omega_{1:n}, \theta_{1:n}, \lambda_0] = \int_{\mathcal{Y} \times \mathcal{T}} (T\kappa - Y)p(Y, T \mid L, A = a, \omega_{1:n}, \theta_{1:n}, \lambda_0) dY dT \quad (4.2)$$

Where integration is over the joint model in (3.1) with $X_i = (A_i, L_i)$. To avoid strong modeling assumptions on the covariate distribution, we use a Bayesian bootstrap [24] estimate of $p(L)$. That is, we model $p(L)$ as a point-mass distribution with mass p_i at the i^{th} observed confounder vector L_i . Specifically, $p(L = l) = \sum_{i=1}^n p_i \cdot \delta_{L_i}(l)$. The Bayesian bootstrap follows from an improper Dirichlet prior on the weights, $p_{1:n} = (p_1, \dots, p_n) \sim Dir(0, \dots, 0)$. By conjugacy, this yields a posterior distribution $p_{1:n} \mid L \sim Dir(1/n, \dots, 1/n)$.

Computation is done at the end of each MCMC iteration. At the end of the m^{th} iteration, we have a set of parameter draws $\{\omega_{1:n}^{(m)}, \theta_{1:n}^{(m)}, \lambda_0^{(m)}\}$. We then take a draw $p_{1:n}^{(m)}$ from $Dir(1/n, \dots, 1/n)$, and substitute both of these into (4.1) compute

$$\Psi^{(m)} \approx \sum_{i=1}^n p_i^{(m)} \left(E[MV \mid A = 1, L_i, \omega_{1:n}^{(m)}, \theta_{1:n}^{(m)}, \lambda_0^{(m)}] - E[MV \mid A = 0, L_i, \omega_{1:n}^{(m)}, \theta_{1:n}^{(m)}, \lambda_0^{(m)}] \right) \quad (4.3)$$

Doing this for all MCMC draws yields M draws from the posterior of the causal estimand $\{\Psi^{(m)}\}_{1:M}$. The mean of these draws can serve as a Bayesian nonparametric point estimate of Ψ and percentiles of the M draws can be used to form credible intervals. The posterior draws can also be used to compute a point on the CEAC for each κ , $P(NMB > 0 \mid D) \approx \frac{1}{M} \sum_m I(\Psi^{(m)} > 0)$. If individual-level estimands are required, Equation (4.2) can be evaluated for particular L_i under both treatments using each of the m posterior parameter draws. The difference would be a draw from the posterior of $\Psi_i = NMB_i(\kappa)$, denoted $\Psi_i^{(m)}$. In the causal literature, these are referred to as conditional average treatment effects (CATEs) or individual treatment effects (ITEs). Across M iterations, we would also have subject-level credible intervals for this estimate. Figure 2a visualizes posterior mean and intervals for each Ψ_i in a synthetic example.

5 Adaptive Subgroup Discovery

The MCMC scheme of Section 3.2 yields posterior draws of latent cost-effectiveness cluster membership, $\{c_i^{(m)}\}_{1:M}$. In this section, we propose using these draws to adaptively discover subgroups of patients with different cost-effectiveness profiles. This is “adaptive” in the sense that the number of clusters is not pre-specified, but grows or shrinks as the model adapts to the data complexity. Subgroup discovery is a policy-relevant endeavor since current CEA practice tends to focuses on marginal, population-level analyses - even if entire subgroups of that target population may be harmed. When heterogeneity is explored, it is often done within subgroups that must be pre-defined (e.g. among Hispanic males). Existing approaches to heterogeneity [15, 16, 17] focus on computing ITEs and use post-hoc heuristic procedures to characterize this heterogeneity. Here, our approach is principled and based fully on the posterior.

Using the given MCMC outputs for subgroup discovery is challenging for two reasons. First, the vector of

cluster assignment labels, $c_{1:n}^{(m)}$, have no meaning across MCMC iterations. This is known as label switching [25, 26]. To illustrate, consider that a new cost-effectiveness cluster forms in iteration $m + 1$ and all subjects previously in another cluster are re-assigned to this new cluster. In this case, even though the assignment has changed, the underlying composition of the cluster did not. As a solution, we propose to keep track of the $n \times n$ adjacency matrix $\mathcal{C}^{(m)}$, where the ij^{th} element is a binary indicator of subject i and j being in the same cost-effectiveness cluster. Note that this is just the vector $c_{1:n}^{(m)}$ re-arranged into a matrix. Taking the elementwise mean of this matrix across the m posterior draws yields a probability matrix $\mathcal{P} = (1/M) \sum_m \mathcal{C}^{(m)}$ where ij^{th} element, \mathcal{P}_{ij} , is the posterior probability of subject i and j being in the same cost-effectiveness cluster. To get a hard clustering assignment, we then search draws, $\{c_{1:n}^{(m)}\}_{1:M}$, for the assignment that is “closest” to \mathcal{P} . That is, we search for $c_{1:n}^* = \arg \min_m \|\mathcal{C}^{(m)} - \mathcal{P}\|$, where $\|\cdot\|$ is some matrix norm. This essentially approximates the posterior mode of the EDP-induced partition, \mathcal{P} . Figure 2b visualizes \mathcal{P} as a weighted graph where each subject is a node and the length of vertices connecting two nodes are inversely proportional to \mathcal{P}_{ij} . Subjects with low posterior probability of being in the same cost-effectiveness cluster are far apart on the graph. Such figures are good tools for assessing uncertainty in posterior mode assignments, c_i^* . For instance, the points between the group of dark red and blue clusters represent subjects with highly uncertain mode assignments. The covariate effects of these subjects look just as similar to the well-separated dark blue points as they do to the well-separated dark red points.

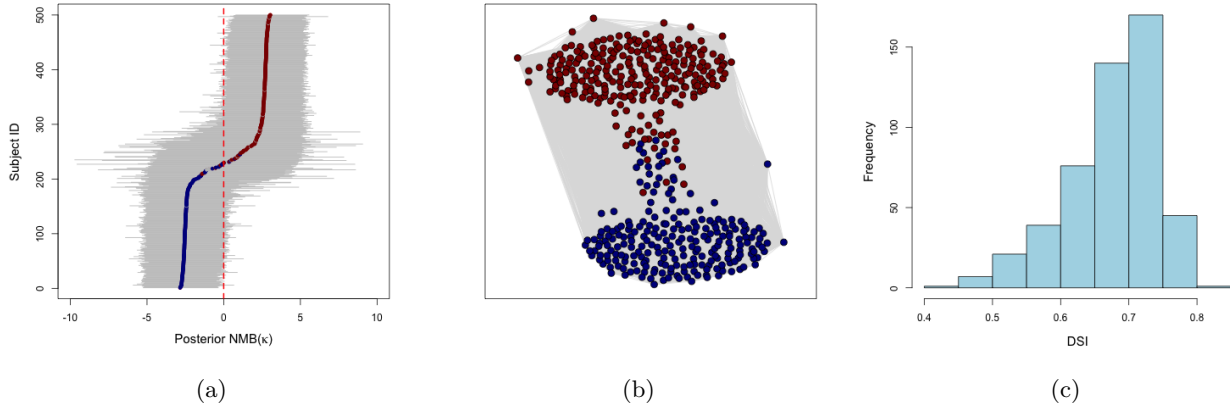


Figure 2: Clustering results from EDP-GP fit using synthetic data with two latent cost-effectiveness clusters. Here, *EDP*-induced clusters on the joint distribution capture differences in *NMB*. Panel 2a shows posterior point and 95% interval estimates Ψ_i (with $\kappa = 1$). Colors indicate posterior model cluster assignment, $c_{1:n}^*$. Panel 2b visualizes the posterior probability matrix \mathcal{P} . Panel 2c is the posterior distribution of *DSI* - indicating that about 70% of the variation in subject-level Ψ_i is explained by the *EDP* clustering.

A second challenge with using the assignments for subgroup discovery is that the *EDP* clusters are not explicitly designed to cluster on *NMB*. The clustering is driven by the complexity of the joint cost-effectiveness distribution. This is necessary for a flexible joint distribution estimate, but may not translate into meaningful *NMB* clusters. For instance, consider a bimodal cost-effectiveness distribution with two groups having very different mean costs. However, the difference in costs between treatment groups in both clusters may be the same. In this case, the *EDP* will likely introduce two clusters with similar *NMBs*. This begs the question: are the clustering results detecting subgroups with different cost-effectiveness (as measured by *NMB*) profiles? To address this concern, we propose a posterior Differential Subgroup Index (*DSI*) that, at each MCMC iteration, computes the proportion of the total variation in $\Psi_i^{(m)}$ that is explained by the cluster partition in that iteration.

First, define the mean *NMB* in subject i 's cluster at iteration m : $\bar{\Psi}_i^{(m)} = \frac{1}{\sum_j I(c_j^{(m)}=c_i^{(m)})} \sum_{j|c_j^{(m)}=c_i^{(m)}} \Psi_j^{(m)}$.

Then the *DSI* measure is,

$$DSI^{(m)} = \frac{\sum_i \left(\bar{\Psi}_i^{(m)} - \Psi^{(m)} \right)^2}{\sum_i \left(\Psi_i^{(m)} - \Psi^{(m)} \right)^2} \quad (5.1)$$

This is intuitive and identical to a regression R^2 statistic. A posterior mean $(1/M) \sum_m DSI^{(m)}$ close to 1 suggests that the *EDP*-induced clustering explains nearly all of the variation in the subject-specific *NMBs*. This implies that the *EDP*-induced clustering at the joint cost-effectiveness level is capturing variation at the *NMB* level. Across the m iterations, we have an entire posterior distribution for this statistic $\{DSI^{(m)}\}_{1:M}$, which reflects our uncertainty about how well the clustering is capturing heterogeneity in *NMB*. Figure 2c plots the posterior distribution for *DSI* for a synthetic example generated with two cost-effectiveness clusters. We can then summarize our data along the mode partition, $c_{1:n}^*$. For instance, in the synthetic example, we can create a table comparing the observed data summaries of the two identified clusters. These can be used to motivate future cost-effectiveness studies targeting these subgroups. We note that we do not attempt to estimate cluster-specific causal effects. Label switching and the fundamental non-identifiability of the cluster assignments complicate this task.

6 Assessing Frequentist Properties via Simulation

Table 1 displays simulation results assessing the frequentist properties of our model's posterior mean and interval estimates for Ψ (Equation 4.1) under a variety of settings. We simulate data with one continuous confounder, a binary treatment, Weibull survival distribution, and Gaussian conditional cost distribution. Data were simulated under low (5%) and high (20%) covariate-dependent censoring. Under the parametric setting, the joint distribution is unimodal. Under the bimodal setting, we simulate with two distinct cost-effectiveness clusters. Figure 3b shows the survival time -confounder scatterplot for one such bimodal dataset. We include the doubly-robust estimator (DR-SL) of Li et al [7] as a comparator. This approach involves estimating separate models for cost and log-survival time via super learner. Predictions from this model are weighted by the inverse probability of treatment and inverse probability of censoring. We estimate the former using a correctly specified logistic regression and the latter with a discrete-time logistic failure time model. We include regression trees, generalized additive and linear models, as well as elastic net generalized linear model in the super learner library. For the *EDP*-GP, we run using independent Gaussian base distributions for G_0 that are null centered with flat priors, relative to the data variance. We set λ_0^* to an exponential (constant) hazard, with uninformative $b = 1e - 6$. We set $\xi = .001$, which is large relative to b . This induces an informative prior AR(1) smoothing, which would likely be desirable in practical scenarios with rapidly declining at-risk counts.

Table 1: Simulation Results. Average bias of posterior mean NMB (as discussed in Section 4) along with coverage and average width of 95% credible/credible (CI) interval is reported for EDP-GP model. Point estimate is reported for the doubly-robust estimator using super learner along with coverage and width of 95% bootstrap BCa interval. Absolute bias is reported a proportion of the true values. Censoring rate was 5% in the low setting and 20% in the high setting. Willingness-to-pay is set to $\kappa = 1$. Results are across 200 simulated datasets with $N = 1000$ subjects each.

Simulation Setting		EDP-GP			DR-SL		
Joint Dist.	Censoring	Bias	Coverage	Width	Bias	Coverage	Width
Parametric	Low	0.019	0.965	0.162	0.001	0.960	0.133
	High	0.010	0.965	0.164	0.010	0.900	0.191
Bimodal	Low	0.012	0.945	0.184	0.139	0.485	0.729
	High	0.012	0.935	0.196	0.183	0.325	0.832

[ADDITIONAL SIMULATIONS PENDING]

Across settings, the posterior mean estimator of Ψ exhibits low bias and the 95% credible interval exhibits close to nominal coverage. Average interval width increases in the bimodal settings, relative to the parametric setting. The DR-SL method performs well in the parametric settings with low and high censoring. Bias increases slightly and coverage slightly declines in this setting as censoring is increased to 20%. In the bimodal setting, bias increases and coverage is no longer close to nominal. Though the treatment model is correctly specified, the poor outcome model fit (see Figure 3a) slows the convergence rate of the DR-SL estimator, resulting in finite-sample bias. Moreover, the discrete-time failure model cannot capture the bi-modality of the survival distribution. This leads to poor weight estimates and, therefore, additional bias and under-coverage.

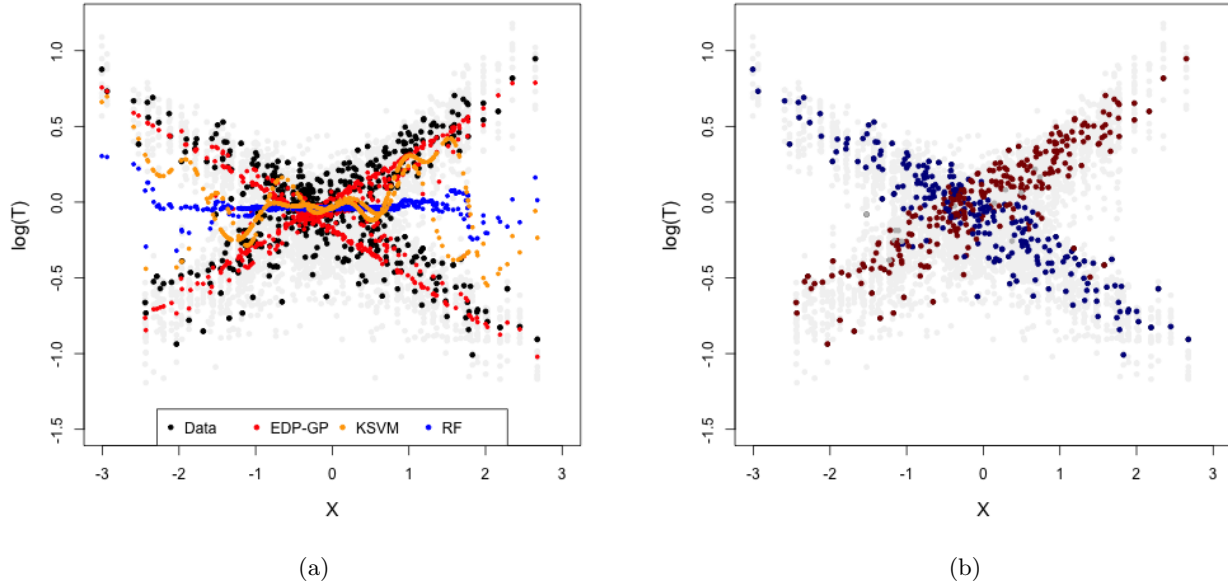


Figure 3: Panel 3a: log survival time, $\log(T)$, posterior mean prediction results from EDP-GP (in red) fit using synthetic data (in black) with covariate, X . Posterior predictive draws from our model (in gray) are shown to convey uncertainty. Predictions from kernelized support vector machine (KSVM) with radial basis function is given in orange. Predictions from random forest (RF) is given in blue. The X-shaped cost-survival relationship is difficult to capture with uni-modal models because it is not a function. The symmetry about the $\log(T)$ axis leads to wild oscillations from one wing of the X to the other in the KSVM and horizontal line through the origin for the RF. Panel 3b: the EDP-GP approximates this shape by introducing two clusters: one with a positive relationship (in dark red) and another with a negative relationship (in dark blue). As shown in Figure 2a, in this synthetic example, this clustering captures differences in NMB.

7 Application to Endometrial Cancer Treatments

[DATA ANALYSIS AND CMS APPROVAL PENDING]

References

- [1] D.Y. Lin, E.J. Feuer, R. Etzioni, and Y. Wax. Estimating medical cost from incomplete data. *Biometrics*, 53(2):419–434, 1997.
- [2] D.Y. Lin. Linear regression analysis of censored medical costs. *Biostatistics*, 1(1):35–47, 2000.
- [3] D. Y. Lin. Regression analysis of incomplete medical cost data. *Statistics in Medicine*, 22(7):1181–1200, 2003.
- [4] Heejung Bang and Anastasios A. Tsiatis. Estimating medical costs with censored data. *Biometrika*, 87(2):329–343, 2000.
- [5] Elizabeth A Handorf, Daniel F Heitjan, Justin E Bekelman, and Nandita Mitra. Estimating cost-effectiveness from claims and registry data with measured and unmeasured confounders. *Statistical Methods in Medical Research*, 28(7):2227–2242, 2019. PMID: 29468944.
- [6] Yijian Huang. Calibration regression of censored lifetime medical cost. *Journal of the American Statistical Association*, 97(457):318–327, 2002.
- [7] Jiaqi Li, Anil Vachani, Andrew Epstein, and Nandita Mitra. A doubly robust approach for costeffectiveness estimation from observational data. *Statistical Methods in Medical Research*, 27(10):3126–3138, 2018.
- [8] Gianluca Baio. Bayesian models for cost-effectiveness analysis in the presence of structural zero costs. *Statistics in Medicine*, 33(11):1900–1913, 2014.
- [9] Yanxun Xu, Peter Müller, Abdus S. Wahed, and Peter F. Thall. Bayesian nonparametric estimation for dynamic treatment regimes with sequential transition times. *Journal of the American Statistical Association*, 111(515):921–950, 2016. PMID: 28018015.
- [10] Dandan Xu, Michael J. Daniels, and Almut G. Winterstein. A bayesian nonparametric approach to causal inference on quantiles. *Biometrics*, 74(3):986–996, 2018.
- [11] Jennifer L. Hill. Bayesian nonparametric modeling for causal inference. *Journal of Computational and Graphical Statistics*, 20(1):217–240, 2011.
- [12] Chanmin Kim, Michael J. Daniels, Bess H. Marcus, and Jason A. Roy. A framework for bayesian nonparametric inference for causal effects of mediation. *Biometrics*, 73(2):401–409, 2017.
- [13] Jason Roy, Kirsten J. Lum, and Michael J. Daniels. A bayesian nonparametric approach to marginal structural models for point treatments and a continuous or survival outcome. *Biostatistics*, 18(1):32–47, 2017.
- [14] Jason Roy, Kirsten J. Lum, Bret Zeldow, Jordan D. Dworkin, Vincent Lo Re, and Michael J. Daniels. Bayesian nonparametric generative models for causal inference with missing at random covariates. *Biometrics*, 0(0), 2018.
- [15] P. Richard Hahn, Jared S. Murray, and Carlos Carvalho. Bayesian regression tree models for causal inference: regularization, confounding, and heterogeneous effects, 2017.

- [16] Nicholas C. Henderson, Thomas A. Louis, Gary L. Rosner, and Ravi Varadhan. Individualized treatment effects with censored data via fully nonparametric bayesian accelerated failure time models, 2017.
- [17] Susan Athey and Stefan Wager. Estimating treatment effects with causal forests: An application, 2019.
- [18] Arman Oganisian, Nandita Mitra, and Jason Roy. A Bayesian Nonparametric Model for Zero-Inflated Outcomes: Prediction, Clustering, and Causal Estimation. *arXiv e-prints*, page arXiv:1810.09494, Oct 2018.
- [19] Sara Wade, David B. Dunson, Sonia Petrone, and Lorenzo Trippa. Improving prediction from dirichlet process mixtures via enrichment. *J. Mach. Learn. Res.*, 15(1):1041–1071, January 2014.
- [20] Luis E. Nieto-Barajas and Stephen G. Walker. Markov beta and gamma processes for modelling hazard rates. *Scandinavian Journal of Statistics*, 29(3):413–424, 2002.
- [21] Radford M. Neal. Markov chain sampling methods for dirichlet process mixture models. *Journal of Computational and Graphical Statistics*, 9(2):249–265, 2000.
- [22] Donald B. Rubin. Bayesian inference for causal effects: The role of randomization. *Ann. Statist.*, 6(1):34–58, 01 1978.
- [23] A new approach to causal inference in mortality studies with a sustained exposure period - application to control of the healthy worker survivor effect. *Mathematical Modelling*, 7(9):1393 – 1512, 1986.
- [24] Donald B. Rubin. The bayesian bootstrap. *Ann. Statist.*, 9(1):130–134, 01 1981.
- [25] David B. Dahl. *Model-Based Clustering for Expression Data via a Dirichlet Process Mixture Model*, page 201?218. Cambridge University Press, 2006.
- [26] Matthew Stephens. Dealing with label switching in mixture models. *Journal of the Royal Statistical Society: Series B (Statistical Methodology)*, 62(4):795–809, 2000.
- [27] Gareth O. Roberts and Jeffrey S. Rosenthal. Optimal scaling for various metropolis-hastings algorithms. *Statist. Sci.*, 16(4):351–367, 11 2001.

A Identification of Causal Net Monetary Benefit

Recall that we are interested in estimating $\Psi = E[MV^1] - E[MV^0]$, where the expectation implicitly conditional on the parameters governing the joint cost-survival distribution. We can identify each term of Ψ . Starting with an iterated expectation over L ,

$$\begin{aligned} E[MV^a] &= E_{\mathcal{L}}[E_{\mathcal{Y},\mathcal{T}}[MV^a \mid L, \omega_{1:n}, \theta_{1:n}, \lambda_0]] \\ &= E_{\mathcal{L}}[E_{\mathcal{Y},\mathcal{T}}[MV^a \mid A = a, L, \omega_{1:n}, \theta_{1:n}, \lambda_0]] \\ &= E_{\mathcal{L}}[E_{\mathcal{Y},\mathcal{T}}[MV \mid A = a, L, \omega_{1:n}, \theta_{1:n}, \lambda_0]] \\ &= \int_{\mathcal{L}} E_{\mathcal{Y},\mathcal{T}}[MV \mid A = a, L, \omega_{1:n}, \theta_{1:n}, \lambda_0] dP(L) \\ &= \int_{\mathcal{L}} \int_{\mathcal{Y},\mathcal{T}} (T\kappa - Y) p(Y, T \mid A = a, L, \omega_{1:n}, \theta_{1:n}, \lambda_0) dP(L) \end{aligned}$$

This yields Equation (4.1). The second line follows from extended conditional ignorability, $Y^a, T^a \perp A \mid L$, allowing us to condition on $A = a$ after first conditioning on L . The third line follows from extended consistency, that is $(Y^a, T^a) = (Y, T) \mid A = a$. These are extensions of the usual conditional ignorability and consistency assumptions. Implicit in the above is the assumption of no joint interference, $(Y_i^{a_{1:n}}, T_i^{a_{1:n}}) = (Y_i^{a_i}, T_i^{a_i})$. That is, each subject's potential outcome vector is independent of others' treatments. Positivity requires no modification, so as usual the treatment probability must be bounded $0 \leq P(A \mid L) \leq 1$ at all levels of L . The expression above identifies a causal estimand that is purely a function of unknown parameters. Thus a posterior distribution over the parameters induces a posterior distribution over monetary value.

B Posterior Computation for Gamma Process

Prior Specification

This appendix provides additional details for updating the baseline hazard model with a dependent Gamma process prior [20]. Much of this is a detailed overview of the results established by Nieto-Barajas and others in their 2002 paper and outlined in documentation of the **BGP Hazard** R package. We provide an abbreviated presentation adapted to the context of our joint model for the reader's convenience.

Consider observing right-censored survival time data for $i = 1, \dots, n$ subjects with survival time T_i and death indicator δ_i . Consider a partition, $\{\tau_v\}_{v=1:V}$, of the time interval such that $0 < \tau_1 < \tau_2 < \dots < \tau_V$ where $\tau_V > \max_i(T_i)$. In this case we consider equally-spaced interval such that $\Delta_v = \tau_v - \tau_{v-1}$ for all v . A piecewise constant hazard model can be defined as

$$\lambda_0(t) = \sum_{v=1}^V \lambda_{0v} I(\tau_{v-1} < t \leq \tau_v)$$

. If *a priori* the baseline hazard $\lambda_0(t) \sim \mathcal{GP}(b\lambda_0^*, b)$, then the hazard rate in each interval follows $\lambda_{0v} \sim \text{Gam}(\frac{1}{b}\lambda_{0v}^*, b)$, where $b = b^*\Delta_v$ and $\lambda_{0v}^* = \Lambda_0^*(\tau_v) - \Lambda_0^*(\tau_{v-1})$. Here, Λ_0 denotes the cumulative hazard. Note that we suppress dependence of b on v since we consider a setting where Δ_v is constant. The dependent Gamma Process of Nieto-Barajas and others follows from introducing latent processes $\{c_v\}_{1:V}$ and $\{u_v\}_{1:V}$. The process is initiated with $\lambda_1 \sim \text{Gam}(\frac{1}{b}\lambda_{01}^*, b)$. Now for $v = 1, 2, \dots$, $u_v \mid \lambda_v, c_v \sim \text{Pois}(c_v\lambda_{0v})$ and

$\lambda_{0v+1} \mid u_v, c_v \sim \text{Gam}(\frac{1}{b}\lambda_{0v+1}^* + u_v, b + c_v)$. The conditional prior mean of this process is

$$E[\lambda_{0v} \mid \lambda_{0v-1}] = \frac{b\lambda_{0v}^* + c_{v-1}\lambda_{0v-1}^*}{b + c_{v-1}}$$

So the prior mean baseline hazard rate in current interval v is a weighted average of the prior baseline hazard rate, λ_{0v}^* , in the current time interval and the prior baseline hazard rate in the previous time interval, λ_{0v-1}^* . This is the induced AR(1) smoothness of the dependent Gamma Process. Following, Nieto-Barajas we place a hyperprior on $\{c_v\}_{1:V}$, assuming $c_v \mid \xi \stackrel{iid}{\sim} \text{Exp}(\xi)$. Where the prior mean is $E[c_v] = \xi$. The magnitude of ξ (relative to b) controls the aggressiveness of the prior AR(1) shrinkage. if $\xi \gg b$, then on average $c_{v-1} \gg b$ at all intervals v , meaning that $E[\lambda_{0v} \mid \lambda_{0v-1}] \approx \lambda_{0v-1}^*$. Similarly, if $\xi \ll b$, then $E[\lambda_{0v} \mid \lambda_{0v-1}] \approx \lambda_{0v}$ - i.e. almost no shrinkage to the previous hazard.

Thus, the notation $\lambda_0 \sim \mathcal{GP}(b\lambda_0^*, b, \xi)$ denotes this prior for the piecewise constant model $\lambda_0(t)$. Specifically, the joint prior is

$$p(\lambda_{01:V}, c_{1:V}, u_{1:V} \mid b^*, \xi) = p(\lambda_1)p(u_1 \mid \lambda_{01}, c_1) \prod_{v=2}^V p(u_v \mid \lambda_v, c_v)p(\lambda_{0v} \mid u_{v-1}, c_{v-1}) \prod_{v=1}^V p(c_v \mid \xi) \quad (\text{B.1})$$

With hyperparameters b and ξ . This can be combined with a Likelihood for the observed data to obtain conditional posteriors for each parameter block.

Likelihood Construction

Now we consider the $\mathcal{GP}(b\lambda_0^*, b, \xi)$ prior for the baseline hazard in a proportional hazard model $\lambda(t \mid X_i, \theta_i) = \lambda_0(t) \exp(X_i' \theta_i)$, where $\lambda_0(t) = \sum_{v=1}^V \lambda_{0v} I(\tau_{v-1} < t \leq \tau_v)$. Specifically, our goal is to find the posterior $p(\{\lambda_{0v}\}_{1:V}, \{c_v\}_{1:V}, \{u_v\}_{1:V} \mid D)$

For convenience in presentation, define $\eta_i = X_i' \theta_i$. Also note that under the piece-wise constant model, the cumulative hazard is $\Lambda_i(t) = \int_0^t \lambda_0(s) e^{\eta_i} ds = \sum_{v=1}^V \lambda_{0v} e^{\eta_i} \Delta_v(t)$. Here, $\Delta_v(t) = (t - \tau_{v-1}) I(t \in (\tau_{v-1}, \tau_v]) + \Delta_v I(t > \tau_v)$.

Conditional on θ_i , standard survival likelihood construction with right-censored data yields

$$p(T_i \mid X_i, \theta_i, \delta_i, \lambda_{01:V}) = \prod_{i \mid \delta_i=1} f(T_i \mid X_i, \theta_i) \prod_{i \mid \delta_i=1} S(T_i \mid X_i, \theta_i)$$

Subjects with an event contribute to the likelihood via the density, f , and censored subjects contributed via the survival function S , both of which can be expressed in terms of the hazard. Denote λ_{0v_i} as the hazard rate of the increment in which subject i died. The density evaluated at subject i 's death time is,

$$f(T_i \mid X_i, \eta_i) = \lambda_0(T_i) e^{-\Lambda_i(T_i)} = \lambda_{v_i} e^{\eta_i} \exp \left\{ - \sum_{v=1}^V \lambda_{0v} e^{\eta_i} \Delta_v(T_i) \right\}$$

The survival function in terms fo the hazard is,

$$S(T_i \mid X_i, \theta_i) = \exp \left\{ - \Lambda_i(T_i) \right\} = \exp \left\{ - \sum_{v=1}^V \lambda_{0v} e^{\eta_i} \Delta_v(T_i) \right\}$$

So the full likelihood is

$$p(T_i | X_i, \theta_i, \delta_i, \lambda_{01:V}) = \left(\prod_{i|\delta_i=1} \lambda_{0v_i} \right) \exp \left\{ \sum_{i|\delta_i=1} \eta_i \right\} \exp \left\{ - \sum_{v=1}^V \lambda_{0v} \left(\sum_{i=1}^n e^{\eta_i} \Delta_v(T_i) \right) \right\} \quad (\text{B.2})$$

Conditional Posterior Updates

The likelihood (B.2) can be combined with the joint prior (B.1) to obtain the following conditional posteriors distributions for $u_{1:V}$, $c_{1:V}$, and $\lambda_{01:V}$. First, the conditional posterior distribution of $\{c_v\}_{1:V}$ is

$$p(c_v | u_v, \lambda_{0v+1}, \lambda_{0v}) \propto \begin{cases} c_v^{u_v} \exp \left\{ - (\lambda_{0v} + \lambda_{0v+1} + \frac{1}{\xi}) c_v \right\} (b + c_v)^{\lambda_{0v+1}^* + u_v} & v = 1, \dots, V-1 \\ \text{Gam}(u_v + 1, \lambda_{0v} + \frac{1}{\xi}) & v = V \end{cases} \quad (\text{B.3})$$

For $v = 1, \dots, V-1$ this update is not conjugate. We sample each c_v separately using Adaptive Metropolis-Hastings with separate proposal variances for each c_v . The proposal variances are tuned every few iterations in the burn-in period to target a 23.4% acceptance rate, which has been shown to be optimal in more than 10 dimensions [27]. The latent process $\{u_v\}_{1:V}$ can be updated from the following conditional posterior,

$$p(u_v | c_v, \lambda_{0v+1}, \lambda_{0v}) \propto \begin{cases} \frac{[c_v \lambda_{0v} \lambda_{0v+1} (b + c_v)]^{u_v}}{\Gamma(u_v + 1) \Gamma(\lambda_{0v+1}^* + u_v)} & v = 1, \dots, V-1 \\ \text{Pois}(c_v \lambda_{0v}) & v = V \end{cases} \quad (\text{B.4})$$

Note here u_v is integer-valued and non-conjugate for $v = 1, \dots, V-1$. To sample from these conditional posteriors, we use grid sampling with a large grid of points $\{0, \dots, 10000\}$. Finally, the conditional posteriors of the hazard rate in each interval is given by

$$p(\lambda_{0v} | -, D) = \begin{cases} \text{Gam}(d_1 + u_1 + \lambda_{01}^*, c_1 + b + \sum_{i=1}^n e^{\eta_i} \delta_1(T_i)) & v = 1 \\ \text{Gam}(d_v + u_v + u_{v-1} + \lambda_{0v}^*, b + c_v + c_{v-1} \sum_{i=1}^n e^{\eta_i} \delta_v(T_i)) & v = 2, \dots, V \end{cases} \quad (\text{B.5})$$

Above, d_v is the number of deaths in interval v . Note that the conditional distribution is fully conjugate for all v and can be sampled directly. Note also that this update is the only Gamma Process update that involves data. The processes $u_{1:V}$ and $c_{1:V}$ are latent and the updates do not involve data - but they do induce a dependence between the λ_{0v} , which now must be updated sequentially and in order.

C Simulation Details

Data Generation

We simulate data as follows. For subject $i = 1, \dots, N$,

- Simulate latent cluster membership: $c_i \sim \text{Ber}(p_c)$ and confounding $L_i \sim N(0, 1)$.
- Simulate treatment: $A_i \sim \text{Ber}(\text{expit}(0 + .1L_i))$.
- Simulate event time: draw a uniform random variable $Z_i \sim \text{Unif}(0, 1)$ and set $\eta_i = (1 - 2c_i)L_i + (0 + 2c_i)A_i$. Draw event time from Weibull proportional hazard as $D_i = (-\log(Z_i) \exp(-\eta_i))^{1/10}$.

- Simulate covariate dependent censoring time: $Z_i \sim Unif(0, 1)$. Simulate survival time from a Weibull proportional hazard as $C_i = (-\log(Z_i) \exp(-\eta_i))^{1/10}$.
- Take another uniform draw $Z_i \sim Unif(0, 1)$ and set censoring as $\delta_i = I(C_i < D_i) \cdot I(Z_i < p_\delta)$. Set observed time $T_i = \min(C_i, D_i)$.
- Simulate Cost up to observed time: $Y_i \sim N(\text{mean} = 5 + 5c_i + .1L_i - 3A_i + 1T_i, \text{sd} = .5)$
- Output observed data $D_i = (Y_i, T_i, \delta_i, L_i, A_i)$.

We simulate with $N = 1000$. In the bimodal setting, $p_c = .5$, leading to $\eta_i = L_i$ for $c_i = 0$ and $\eta_i = -1L_i + 2A_i$ for $c_i = 1$. Among $c_i = 1$, treated subjects ($A_i = 1$) have worse survival. There is no differential treatment effect on survival among $c_i = 0$. Since survival time T_i appears in the cost model, this bi-modality follows through to the cost distribution. In the parametric settings, we set $p_c = 0$. We set $p_\delta = .4$ in the high setting to target 20% censoring and $p_\delta = .1$ in the low setting to target 5% censoring.

D Data Analysis Details

[DATA ANALYSIS AND CMS APPROVAL PENDING]